ELSEVIER

Biochemical Pharmacology 64 (2002) 1447–1460

Biochemical Pharmacology

Molecular cloning and characterization of mouse CYP2J6, an unstable cytochrome P450 isoform

Jixiang Ma[a], J. Alyce Bradbury[a], Lorraine King[a], Robert Maronpot[a], Linda S. Davis[b], Matthew D. Breyer[b], Darryl C. Zeldin[a,*]

[a]*Division of Intramural Research, National Institute of Environmental Health Sciences, 111 T.W. Alexander Drive, Building 101, Research Triangle Park, NC 27709, USA*
[b]*Department of Medicine, Vanderbilt University, Nashville, TN 37232, USA*

Received 7 December 2001; accepted 22 April 2002

Abstract

A cDNA encoding a new cytochrome P450 was cloned from a mouse liver library. Sequence analysis revealed that this 2046-bp cDNA encodes a 501-amino acid polypeptide that is 72–94% identical to other CYP2J subfamily P450s and is designated CYP2J6. Northern analysis demonstrated that CYP2J6 transcripts are abundant in the small intestine and present at lower levels in other mouse tissues. *In situ* hybridization revealed that CYP2J6 mRNAs are present in luminal epithelial cells of the gastrointestinal mucosa. The CYP2J6 cDNA was expressed in *Sf*9 cells using baculovirus. The heterologously expressed CYP2J6 protein displayed a typical P450 CO-difference spectrum; however, the protein was unstable as evidenced by the loss of the Soret maxima at 450 nm and the appearance of a 420 nm peak when CYP2J6-expressing cells were disrupted by mechanical homogenization, sonication, or freeze–thaw. Immunoblotting of mouse microsomes with the anti-human CYP2J2 IgG, which cross-reacts with rodent CYP2Js, demonstrated the presence of multiple distinct murine CYP2J immunoreactive proteins in various tissues. Immunoblotting with an antibody to a CYP2J6-specific peptide detected a prominent 55–57 kDa protein in *Sf*9 cell extracts expressing recombinant CYP2J6 but did not detect a protein of similar molecular mass in mouse small intestinal microsomes. Mixing experiments demonstrated that recombinant CYP2J6 is degraded rapidly in the presence of small intestinal microsomes consistent with proteolysis at highly sensitive sites. *Sf*9 cells, which express both CYP2J6 and NADPH-P450 oxidoreductase, metabolized benzphetamine but not arachidonic acid. We conclude that CYP2J6 is an unstable P450 that is active in the metabolism of benzphetamine, but not arachidonic acid.
Published by Elsevier Science Inc.

Keywords: Cytochrome P450; Benzphetamine; Gastrointestinal tract; Epithelial cells; *In situ* hybridization; Baculovirus

1. Introduction

The cytochromes P450 constitute a large superfamily of heme-thiolate proteins that catalyze the oxidation of a wide variety of substrates, including xenobiotics and endogenous lipids [1]. The 18 known mammalian P450 gene families are divided into 43 subfamilies, each comprised of one or more individual P450 genes. Rabbit CYP2J1, the first member of the mammalian CYP2J subfamily, was originally purified from small intestinal microsomes and later cloned from a small intestine cDNA library [2,3]. More recently, several members of the CYP2J subfamily have been cloned from other species, including human (CYP2J2), rat (CYP2J3 and CYP2J4), and mouse (CYP2J5 and CYP2J9) [4–8] as reviewed by Scarborough and co-workers [9]. The CYP2J mRNAs and proteins have been found at high levels in liver and in extrahepatic tissues including the heart, kidney, intestine, pancreas, brain, and lung, suggesting that these P450 enzymes may have important physiological functions [9]. In this regard, CYP2J enzymes catalyze the NADPH-dependent oxidation of arachidonic acid to *cis*-epoxyeicosatrienoic acids (EETs), mid-chain *cis-trans*-conjugated dienols (HETEs), and ω-terminal alcohols of arachidonic acid [4–8]. The EETs are endogenous

* Corresponding author. Tel.: +1-919-541-1169; fax: +1-919-541-4133.
E-mail address: zeldin@niehs.nih.gov (D.C. Zeldin).

Abbreviations: P450, cytochrome P450; EET, epoxyeicosatrienoic acid; HETE, hydroxyeicosatetraenoic acid; CYPOR, NADPH-cytochrome P450 oxidoreductase; *Sf*, *Spodoptera frugiperda*; PMSF, phenylmethylsulfonyl fluoride; RT–PCR, reverse transcriptase–polymerase chain reaction.

0006-2952/02/$ – see front matter. Published by Elsevier Science Inc.
PII: S0006-2952(02)01393-X

constituents of numerous tissues and possess a variety of potent biological activities. For example, EETs have been shown to control peptide hormone secretion in pancreas, pituitary, and hypothalamus [10,11], regulate vascular tone in the intestine and brain [12,13], affect ion transport and airway smooth muscle tone in the lungs [14,15], improve functional recovery following global ischemia in the heart [5], and modulate nuclear factor-κB (NF-κB) activity in the vascular endothelium [16]. And recently, the CYP2J enzymes have been shown to bioactivate all-*trans*- and 9-*cis*-retinal to the corresponding retinoic acids [17]and metabolize linoleic acid to leukotoxins and hydroxyoctadecadienoic acids [18].

Since the gastrointestinal tract is directly exposed to food and drugs, it has been suggested that intestinal P450s are involved in the biotransformation of dietary nutrients, orally ingested toxicants, procarcinogens, and other xenochemicals [19]. Although several P450 isoforms have been found in the intestine, rabbit CYP2J1 and rat CYP2J4 appear to be unique in that they are expressed *predominantly* in the small intestine [3,6,17]. In addition, a second intestinal-specific CYP2J isoform was purified from rabbit small intestine and shown to share immunologic, spectral, and catalytic properties with CYP2J1 [20]. In contrast, human CYP2J2 mRNA and protein were shown to be abundant throughout the entire gastrointestinal tract from esophagus to colon [21]. In addition to their role in the metabolism of endogenous substances, the CYP2J enzymes are active in the metabolism of xenobiotics. Thus, CYP2J1 metabolizes aminopurine, benzphetamine, and *N*,*N*-dimethylaniline, CYP2J2 is active against diclofenac and bufuralol, CYP2J3 metabolizes benzphetamine, and CYP2J4 exhibits low activity toward warfarin [2,3,5,6,9]. Importantly, recent data suggest that intestinal CYP2J4 mRNA and protein levels are induced by pyrazole and, to a lesser extent, by phenobarbital [22], whereas fasting down-regulates rat intestinal CYP2J protein expression.[1]

Given the putative role of CYP2Js in the metabolism of xenochemicals and endogenous lipids, it is of importance to further characterize the biochemical and molecular properties of these P450s and to develop specific immunologic and molecular probes. Herein, we report the cDNA cloning and heterologous expression of a new mouse P450, designated CYP2J6. CYP2J6 transcripts were most abundant in the small intestine but also present in extraintestinal tissues. In the intestine, CYP2J6 mRNAs were expressed predominantly in luminal epithelial cells. The recombinant protein displayed typical P450 spectral characteristics but was unstable *in vitro*, suggesting that enzyme activity may be regulated at the post-translational level. We also provide immunologic evidence for the presence of multiple CYP2J isoforms in mouse tissues.

[1] Qu W and Zeldin DC, unpublished observations.

2. Materials and methods

2.1. Materials

[α-^{32}P]dATP and [1-^{14}C]arachidonic acid were purchased from DuPont-New England Nuclear. Restriction enzymes were purchased from New England Biolabs. PCR reagents were purchased from the Perkin-Elmer Corp. Oligonucleotides were purchased from Life Technologies. All other chemicals and reagents were purchased from the Sigma-Aldrich Chemical Co., unless otherwise specified. Adult male and female C57BL/6J mice were obtained from the Jackson Laboratory.

2.2. cDNA cloning and sequence analysis

A Lambda ZAP B6/CBAF1J male mouse liver cDNA library (Stratagene) was screened with the 1.8-kb CYP2J3 cDNA probe as described previously [7]. Approximately 100 positive clones were identified, of which 21, selected at random, were plaque-purified and rescued into pBluescript (Stratagene). The cDNA inserts were partially sequenced by the dideoxy chain termination method, using Sequenase® version 2.0 (U.S. Biochemical) and universal T3/T7 oligonucleotide primers. Nucleotide sequences were analyzed by searching the GenBank and EMBL database, utilizing GCG software (Genetics Computer Group, Inc.). Sixteen of the 21 selected clones contained sequences that were identical to CYP2J5 [7]. Four of the remaining clones contained the same sequences and were >70% identical to previously identified CYP2J cDNAs. One of these four clones (clone JM-15) was completely sequenced utilizing a total of 20 oligonucleotide primers (21–25 nucleotides, each) that spanned the entire length of the sense and antisense cDNA strands. The novel cDNA sequence (2046 bp) represented by clone JM-15 was submitted to the Committee on Standardized Cytochrome P450 Nomenclature and has been designated CYP2J6. This sequence has also been submitted to GenBank and assigned the accession number U62295.

2.3. Heterologous expression of recombinant CYP2J6

The CYP2J6 cDNA was expressed alone or co-expressed with CYPOR in *Sf*9 insect cells using methods similar to those described for CYP2J2, CYP2J3, CYP2J5, and CYP2J9 [4,5,7,8]. The CYP2J6 cDNA including the entire coding region (nucleotides 248–1803) was subcloned into the pBlueBacIV (Invitrogen) and modified pAcUW51-CYPOR expression vectors, and the identity of the resulting constructs was confirmed by direct sequencing. The pAcUW51-CYPOR vector contains the human CYPOR cDNA downstream from the P10 promoter. Cultured *Sf9* cells were co-transfected with either the pAcUW51-CYPOR-CYP2J6 or the pBlueBacIV-CYP2J6 vector and linear wild-type BaculoGold viral DNA, and the recombinant viruses were purified as described previously [7,8].

Cultured *Sf9* cells were infected with high titer baculovirus stock in the presence of δ-aminolevulinic acid and iron citrate (100 μM each). Cells expressing recombinant P450 proteins were harvested 72 hr after infection and lysed in a buffer containing 0.1 M sodium phosphate (pH 7.2), 20% glycerol, 0.2% Emulgen 911 (KAO Chemicals), 1 mM PMSF, 0.1 μg/mL of leupeptin, and 0.04 U/mL of aprotinin (PGE buffer). P450 spectra were obtained according to the method of Omura and Sato [23] using a Shimadzu UV-3000 dual-wavelength/double-beam spectrophotometer (Shimadzu Scientific Instruments). The stability of recombinant CYP2J6 protein was assessed by a combination of immunoblotting and spectral analysis of the following: (i) CYP2J6-expressing cells disrupted by (a) mechanical homogenization in a buffer containing 0.01 M Tris–Cl (pH 7.5), 0.25 M sucrose, 0.1 μg/mL of leupeptin, 0.04 U/mL of aprotinin, and 1 mM PMSF, (b) sonication in a buffer containing 137 mM NaCl, 2.68 mM KCl, 8 mM Na_2HPO_4, 1.5 mM KH_2PO_4 (pH 7.4), 0.1 μg/mL of leupeptin, 0.04 U/mL of aprotinin, and 1 mM PMSF, or (c) lysis in a buffer containing 0.1 M sodium phosphate (pH 7.4), 20% glycerol, 0.5 to 1.2% sodium cholate, 0.1 mM EDTA, 0.1 mM dithiothreitol, 0.1 μg/mL of leupeptin, 0.04 U/mL of aprotinin, and 1 mM PMSF; and (ii) microsomes prepared from CYP2J6-expressing cells subjected to (a) repeated freezing at −80° and thawing at room temperature, (b) incubation at room temperature for up to 96 hr, and (c) incubation in the presence of mouse small intestinal cytosol, microsomes, or buffer alone for 1–24 hr at 37°.

2.4. Northern blot hybridization

Tissues were collected from untreated adult male C57BL/6J mice killed by lethal CO_2 inhalation. RNA was prepared by the guanidinium thiocyanate/cesium chloride density gradient centrifugation method as described previously [24]. The northern blotting procedure was exactly as described [7] except that the probes used were either the cloned 2046-bp CYP2J6 cDNA insert or a CYP2J6 sequence-specific oligonucleotide (5′-CGGTAGCAGCGAGCATGGCTAGGACTGCAGCTGGT-3′, complementary to nucleotides 229-263 of the CYP2J6 cDNA).

2.5. RT–PCR analysis

RT–PCR was performed on male mouse tissue RNAs using the GeneAmp® RNA PCR Kit (Perkin-Elmer) exactly as described in the instruction manual of the manufacturer. The following CYP2J6 sequence-specific oligonucleotides were used: forward primer, 5′-GCGAGCTTGCCTGGGAGAACAACT-3′, corresponding to nucleotides 1579–1602 of the CYP2J6 cDNA; reverse primer, 5′-GTTAAGTTAAATTACGTGAAACAAACCTTC-3′, complementary to nucleotides 1993–2022 of the CYP2J6 cDNA. The β-actin specific primers used were as described previously [7]. Control studies demonstrated that the CYP2J6 primers amplified a 444-bp fragment with CYP2J6 cDNA as the template but formed no products with the CYP2J5 cDNA template.

2.6. In situ hybridization

Radiolabeled sense and antisense RNA probes to the full-length mouse CYP2J6 were transcribed from the linearized pBluescript/CYP2J6 construct using T7 and T3 RNA polymerases and [α-^{35}S]UTP. The ^{35}S-labeled probes were then subjected to alkaline hydrolysis. *In situ* hybridization was performed on 4% paraformaldehyde-fixed, paraffin-embedded mouse stomach, small intestine, uterus, kidney, brain, and lung tissue sections as previously described [25].

2.7. Production of polyclonal antibodies and immunoblotting

Production and affinity purification of the rabbit anti-human CYP2J2 IgG have been described [4]. This antibody cross-reacts with known CYP2J P450s but not with members of the CYP1A, CYP2A, CYP2B, CYP2C, CYP2D, CYP2E, or CYP4A subfamilies [4,5,7,8,16]. A peptide corresponding to amino acids 103–117 of the deduced CYP2J6 amino acid sequence was designed based upon sequence alignments with CYP2J5 and other known CYP2 family P450s. The peptide was synthesized and HPLC-purified by the Protein Chemistry Facility at the University of North Carolina, and coupled to keyhole limpet hemocyanin via a carboxyl-terminal cysteine to enhance antigenicity. Polyclonal antibodies against this CYP2J6-specific peptide (anti-CYP2J6pep IgG) were raised in New Zealand white rabbits as described [7]. The anti-CYP2J6pep IgG was purified with affinity columns coupled to the immunogenic peptide using a Sulfo-Link kit (Pierce). Microsomal fractions were prepared from adult C57BL/6J mouse tissues, uninfected *Sf*9 insect cells, or *Sf*9 insect cells infected with recombinant CYP2J2 [4], CYP2J5 [7], or CYP2J6 baculovirus by differential centrifugation at 4°. For some experiments, mice received 200 mg pyrazole/kg body weight per day for 3 days via either oral or intraperitoneal routes or vehicle (phosphate-buffered saline) prior to being killed. Western blotting and protein concentration determinations were performed as described previously [4] except that 12% Tris-glycine gels were used (Novex).

2.8. Enzymatic characterization

*Sf*9 insect cells infected with either recombinant CYP2J5 [7] or CYP2J6 baculovirus were resuspended in phosphate-buffered saline ($3-5 \times 10^7$ cells/mL) and incubated with [1-^{14}C]arachidonic acid (55 μCi/μmol; 30–50 μM, final concentration) with constant stirring at 37°.

After 1 hr, aliquots were withdrawn, and the reaction products were extracted into diethyl ether and analyzed by reverse-phase HPLC as described [4]. Products were identified by comparing their reverse-phase HPLC properties with those of authentic standards. Control studies included incubations of uninfected *Sf9* cells and baculovirus-infected *Sf9* cells expressing recombinant CYPOR but containing no spectrally evident P450 with the radiolabeled fatty acid. The benzphetamine *N*-demethylase activity of recombinant CYP2J6 was assessed under identical reaction conditions but employing benzphetamine (2 mM, final concentration) as the substrate. The reaction product (formaldehyde) was quantified according to the method of Nash [26]. Incubations containing uninfected *Sf*9 cells or *Sf*9 cells expressing CYPOR but without spectrally evident P450 were used as controls. The sensitivity of the formaldehyde colorimetric assay was 10^{-6} M.

3. Results

3.1. CYP2J6 cDNA cloning and sequence analysis

Screening of the mouse liver cDNA library with the rat CYP2J3 cDNA probe yielded four clones that contained identical sequences that were different from that of mouse CYP2J5 and CYP2J9 [7,8]. One of these clones (clone JM-15) was selected for further study. Complete nucleic acid sequence analysis of clone JM-15 revealed that the cDNA was 2046 nucleotides long, contained an open reading frame between nucleotides 248 and 1750 flanked by initiation (ATG) and termination (TGA) codons, a 247-nucleotide 5′-untranslated region, and a 296-nucleotide 3′-untranslated region with a polyA tail (Fig. 1). The cDNA encoded a 501-amino acid polypeptide with a calculated molecular mass of 57,819 Da. The deduced amino acid sequence for JM-15 contained a putative heme binding peptide (FSMGKRACLGEQLA) with the underlined conserved residues and the invariant cysteine at position 447. The polypeptide encoded by JM-15 also contained other typical structural features associated with CYP2 family P450s, such as an amino-terminal hydrophobic peptide and a proline cluster between residues 40 and 51 (Fig. 1). A comparison of the deduced JM-15 amino acid sequence with that of other P450s indicated that it was (a) <33% identical to members of the CYP1, CYP3, CYP4, CYP5, CYP6, and CYP7 families, (b) 40–44% identical with several CYP2 family P450s, and (c) 72–94% identical to previously identified CYP2J P450s [3–8]. Based on the amino acid sequence similarity with CYP2J subfamily members, the new mouse heme-thiolate protein was designated CYP2J6 by the Committee on Standardized Cytochrome P450 Nomenclature [1]. Comparison of the deduced CYP2J6 amino acid sequence with that of other CYP2Js revealed modest (72–78%) similarity with CYP2J1, CYP2J2, CYP2J3, CYP2J5, and CYP2J9 but relatively high (94%) percent identity with rat CYP2J4. Furthermore, most of the differences between CYP2J4 and CYP2J6 represented conservative changes (i.e. replacement with residues with overall similar chemical properties) and generally occurred outside of the six putative substrate recognition sites.

3.2. Tissue distribution of CYP2J6 mRNAs

The tissue distribution of CYP2J6 mRNAs was examined by northern analysis. Total RNAs extracted from various mouse tissues were blot hybridized with either the full-length CYP2J6 cDNA probe or a CYP2J6 sequence-specific oligonucleotide under high stringency conditions. As shown in Fig. 2A, the CYP2J6 cDNA hybridized with small intestinal RNA to produce a prominent 2.1-kb transcript, consistent with the predicted size of the full-length CYP2J6 mRNA. This 2.1-kb transcript was also present at lower levels in other mouse tissues including liver, kidney, colon, and to a lesser extent brain, heart, and lung, but was not detectable in testes and skeletal muscle. A much less intense 4.2-kb band was also observed, most prominently in small intestine and at lower levels in other mouse tissues. The identity of this transcript remains unknown, but it may represent an alternate splicing variant of CYP2J6 or another mouse P450 isoform that shares nucleic acid sequence similarity with CYP2J6. Identical results were obtained using the CYP2J6 sequence-specific oligonucleotide probe (data not shown). The broad tissue distribution of CYP2J6 was independently confirmed by RT–PCR analysis of various mouse tissue RNAs using sequence-specific primer pairs. As shown in Fig. 2B, a DNA fragment of the predicted size (444 bp) was amplified from reverse-transcribed small intestine, lung, liver, kidney, and, to a lesser extent, heart RNAs. CYP2J6 fragments were also amplified from stomach, colon, testes, skeletal muscle, and brain RNAs (data not shown). The presence of CYP2J6 mRNAs in the heart was confirmed by screening a mouse heart cDNA library with a human CYP2J2 cDNA probe. All of the four duplicate positive clones isolated by screening 1 million plaques contained sequences that were identical to CYP2J6.

3.3. Cellular localization of CYP2J6 transcripts by in situ hybridization

To examine the cellular localization of CYP2J6 mRNAs within the gastrointestinal tract, we performed *in situ* hybridization of paraformaldehyde-fixed, paraffin-embedded mouse intestinal sections with an ^{35}S-labeled CYP2J6-specific antisense riboprobe. Within the glandular stomach, labeling was present throughout the mucosa with heavy deposits in epithelial cells lining the lumen (Fig. 3A and B). Only background labeling was present in the muscularis layer. Similarly, within the small intestine (jejunum), labeling was most evident overlying the apical

```
   1   G TTG GGG ATA TGA TCC GCA GAA CTC GGT TAG ATG AGC TAA CTT CTT TTA ACC TTG GTT TGA GTC TTT GGA CTT
  74 CCT GCG AGA GCC CAG CTC CAG GGA GGA AAC CAG AGG AGC AAA GGG GAG TGG ACA GAA AGG GAT AGG GAG GGA CTG
 149 AGG GGA CCG GTT TTT AGA AGG GTG CCC CTG TTG TTA GCA CCT GGG ACT TGC CGC AGC TCA GAC CTT CAT TCC TCA
 224 GAC GAA CCA GCT GCA GTC CTA GCC ATG CTC GCT GCT ACC GGC TCC TTG TTA GCC ACG ATC TGG GCA GCG CTC CAT
   1                               M   L   A   A   T   G   S   L   L   A   T   I   W   A   A   L   H
 299 CCC AGG ACT CTG TTG GTG GCT GCA GTC ACC TTC CTG CTT CTG GCT GAT TAC TTC AAA AAC CGG CGC CCC AAG AAC
  18  P   R   T   L   L   V   A   A   V   T   F   L   L   L   A   D   Y   F   K   N   R   R   P   K   N
 374 TAT CCC CCA GGG CCT TGG GGT CTG CCT TTC GTG GGC AAC ATA TTC CAG TTG GAC TTT GGG CAG CCC CAC CTC TCA
  43  Y   P   P   G   P   W   G   L   P   F   V   G   N   I   F   Q   L   D   F   G   Q   P   H   L   S
 449 ATC CAG CCG TTG GTG AAG AAA TAT GGG AAT ATT TTT AGC CTG AAT CTT GGT GAC ATA ACT TCA GTG GTC ATA ACT
  68  I   Q   P   L   V   K   K   Y   G   N   I   F   S   L   N   L   G   D   I   T   S   V   V   I   T
 524 GGA CTG CCC TTA ATC AAA GAA GCA CTT ACT CAA ATG GAA CAA AAC ATT ATG AAT CGT CCT CTA AGT GTT ATG CAA
  93  G   L   P   L   I   K   E   A   L   T   Q   M   E   Q   N   I   M   N   R   P   L   S   V   M   Q
 599 GAA CGT ATA TCT AAT AAA AAT GGA TTG ATC TTC TCC AGT GGC CAA ATA TGG AAG GAG CAA AGA AGG TTT GCC CTG
 118  E   R   I   S   N   K   N   G   L   I   F   S   S   G   Q   I   W   K   E   Q   R   R   F   A   L
 674 ATG ACA CTG AGG AAC TTT GGA CTG GGA AAG AAG AGC TTA GAG GAG CGC ATG CAG GAG GAG GCC TCC CAC CTA GTG
 143  M   T   L   R   N   F   G   L   G   K   K   S   L   E   E   R   M   Q   E   E   A   S   H   L   V
 749 GAA GCC ATA AGA GAG GAG GAA GGA AAA CCT TTC AAC CCT CAC TTC AGT ATC AAC AAT GCA GTT TCC AAT ATC ATT
 168  E   A   I   R   E   E   E   G   K   P   F   N   P   H   F   S   I   N   N   A   V   S   N   I   I
 824 TGC TCT GTC ACC TTT GGG GAG CGC TTT GAC TAC CAT GAC AGT AGA TTT CAG GAG ATG CTG AGG TTA CTG GAC GAG
 193  C   S   V   T   F   G   E   R   F   D   Y   H   D   S   R   F   Q   E   M   L   R   L   L   D   E
 899 GTT ATG TAT TTG GAG ACA ACA ATG ATT AGT CAG CTG TAT AAT ATT TTT CCA TGG ATA ATG AAA TAC ATC CCT GGA
 218  V   M   Y   L   E   T   T   M   I   S   Q   L   Y   N   I   F   P   W   I   M   K   Y   I   P   G
 974 TCA CAT CAA AAA GTT TTC AGA AAC TGG GAA AAA CTG AAA TTG TTT GTC TCT TGT ATG ATT GAT GAT CAC CGG AAA
 243  S   H   Q   K   V   F   R   N   W   E   K   L   K   L   F   V   S   C   M   I   D   D   H   R   K
1049 GAC TGG AAC CCC GAT GAA CCA AGA GAC TTC ATT GAT GCT TTC CTC AAG GAA ATG ACA AAG TAC CCA GAG AAG ACT
 268  D   W   N   P   D   E   P   R   D   F   I   D   A   F   L   K   E   M   T   K   Y   P   E   K   T
1124 ACA AGT TTC AAT GAA GAA AAC CTT ATC TGC AGC ACT TTG GAC CTC TTC TTT GCT GGA ACA GAG ACA ACA TCA ACT
 293  T   S   F   N   E   E   N   L   I   C   S   T   L   D   L   F   F   A   G   T   E   T   T   S   T
1199 ACA TTA CGC TGG GCT CTG CTC TAC ATG GCC CTC TAC CCA GAA GTC CAA GAA AAA GTA CAG GCA GAG ATT GAT AGG
 318  T   L   R   W   A   L   L   Y   M   A   L   Y   P   E   V   Q   E   K   V   Q   A   E   I   D   R
1274 GTG ATT GGC CAG AAG AGG GCA GCA AGA CTT GCT GAT AGA GAA TCC ATG CCC TAT ACC AAT GCT GTC ATC CAC GAG
 343  V   I   G   Q   K   R   A   A   R   L   A   D   R   E   S   M   P   Y   T   N   A   V   I   H   E
1349 GTG CGG AGG ATG GGC AAT ATC ATC CCC TTG AAT GTT CCC AGG GAA GTA GCA ATG GAT ACC AAT TTG AAT GGA TTT
 368  V   R   R   M   G   N   I   I   P   L   N   V   P   R   E   V   A   M   D   T   N   L   N   G   F
1424 CAT CTG CCA AAG GGT ACA ATG GTT CTA ACA AAC CTA ACT GCA CTG CAC AGA GAC CCA AAA GAG TGG GCC ACT CCA
 393  H   L   P   K   G   T   M   V   L   T   N   L   T   A   L   H   R   D   P   K   E   W   A   T   P
1499 GAT GTG TTC AAT CCA GAG CAC TTT TTG GAG AAT GGA CAG TTT AAG AAG AGA GAA TCC TTT CTG CCC TTC TCA ATG
 418  D   V   F   N   P   E   H   F   L   E   N   G   Q   F   K   K   R   E   S   F   L   P   F   S   M
1574 GGA AAG CGA GCT TGC CTG GGA GAA CAA CTG GCC AGG TCT GAG CTG TTC ATT TTC TTC ACT AGC CTT ATG CAA AAA
 443  G   K   R   A   C   L   G   E   Q   L   A   R   S   E   L   F   I   F   F   T   S   L   M   Q   K
1649 TTC ACC TTC AAT CCC CCA ATC AAT GAG AAG CTG AGC CCA AAG TTC AGA AAT GGC CTC ACA CTT TCT CCA GTC AGC
 468  F   T   F   N   P   P   I   N   E   K   L   S   P   K   F   R   N   G   L   T   L   S   P   V   S
1724 CAC CGC ATC TGT GCT GTC CCT AGA CAG TGA TGC TGG AGA AGC AAT GAG AAA AGG AAG ATA AGA TGT AAG GCC TGA
 493  H   R   I   C   A   V   P   R   Q   *
1799 AGC TTC TGG GTT GCT CAC ACG AGA GAA GAA AGA TGT CAG AAA AGG AAG GTG ATT CAA GAA GTA CTG AAG AAA TGT
1874 GGC TTA GAA AAT TGA AGC AAT CTC CTA GAA TAG TAG CCC CTT GAT TTG GTG GTG GGC ACA TCA TTT ATG AGC TCA
1949 GTG GCA TGC CTT TTC ATC TAA ATG TTT TGA GGA TAA TGG TGA TTC TTC CAA ACA AAG TGC ATT AAA TTG AAT TGA
2024 AAA TGA AAA AAA AAA AAA AAA AA
```

Fig. 1. Nucleotide and deduced amino acid sequence for mouse CYP2J6. The putative heme-binding peptide is underlined, and the conserved residues are in bold. An asterisk marks the termination codon. The location of the peptide used to prepare the anti-CYP2J6pep IgG is enclosed within a box.

cytoplasm of epithelial cells lining the villi, and was also present, albeit at lower levels, in the glandular crypts (Fig. 3D and E). There was no significant difference in the abundance or localization of intestinal labeling between male and female mice. In contrast, hybridization of stomach and small intestine sections with the sense RNA probe yielded only background signal that was similar to non-tissue areas of the slide, thus, demonstrating the

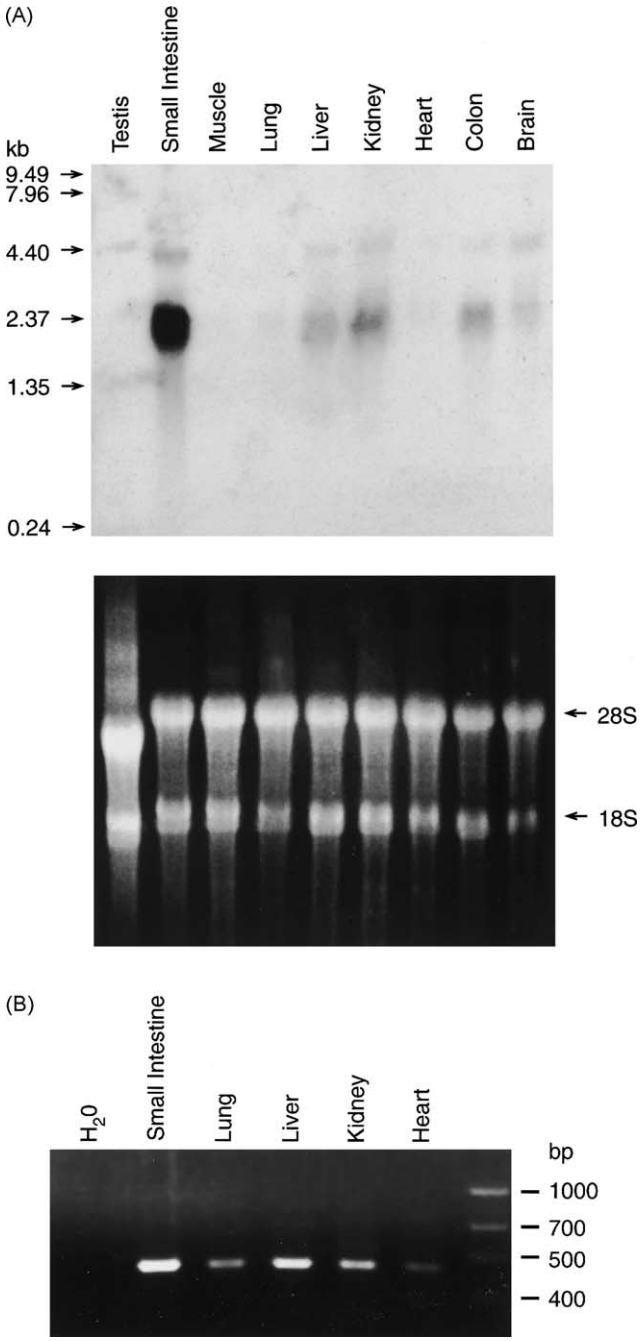

Fig. 2. Tissue distribution of CYP2J6 mRNA by northern analysis and RT–PCR. (A) Total RNA (25 μg/lane) isolated from various mouse tissues was denatured and electrophoresed in a 1.2% agarose gel containing 2.2 M formaldehyde. After capillary-pressure transfer to Hybond-N^+ membranes, the blot was hybridized with the full-length CYP2J6 cDNA labeled with [α-^{32}P]dATP by nick translation. Top: autoradiograph of blot after a 24-hr exposure time. Bottom: ethidium bromide stained gel before transfer. (B) Total RNA (1 μg) was reverse-transcribed and then PCR-amplified using CYP2J6-specific primer pairs as described in Section 2. PCR products were electrophoresed on 1.2% agarose gels containing ethidium bromide.

specificity of the hybridization for the CYP2J6 mRNA (Fig. 3C and F). We observed only minimal diffuse labeling in other mouse tissues including the kidney, lung, and brain (data not shown). Interestingly, the CYP2J6 antisense RNA probe produced intense labeling in epithelial cells lining the female uterus lumen and in endometrial glands (Fig. 3G and H). Under identical conditions, the sense RNA probe yielded only uniform background staining (Fig. 3I).

3.4. Heterologous expression of recombinant CYP2J6

The coding region of CYP2J6 cDNA was inserted into both the pBlueBacIV and modified pAcUW51-CYPOR transfer vectors, and the identity of the resulting constructs was confirmed by direct sequencing. The protein encoded by CYP2J6 was then expressed with/without human CYPOR in *Sf*9 insect cells using the baculovirus system. The level of expression of recombinant CYP2J6 was ~20 nmol P450/L of infected *Sf*9 cells using the pBlueBacIV vector. As observed previously for CYP2J3, CYP2J5, and CYP2J9 [5,7,8], CYP2J6 expression was significantly lower (3–4 nmol P450/L of infected *Sf*9 cells) in the presence of CYPOR when the pAcUW51-CYPOR transfer vector was used. Coomassie Brilliant Blue-stained SDS–polyacrylamide gels of the lysate of CYP2J6-expressing *Sf*9 cells showed an abundant protein band with an estimated molecular mass of 55–57 kDa that was not present in uninfected *Sf*9 cell lysates (data not shown).

Immunoblot analysis of microsomes prepared from *Sf*9 cells infected with recombinant CYP2J6 baculovirus stock indicated that the heterologously expressed CYP2J6 protein was recognized by the anti-CYP2J2 IgG (Fig. 4A). Given that this antibody has been shown to immunoreact with CYP2J2, CYP2J3, CYP2J5, and CYP2J9 but not with non-CYP2J P450s [4,5,7,8,16], these data provide direct evidence that the expressed CYP2J6 protein shares immunological characteristics with the other CYP2Js. We also prepared a polyclonal antibody to a CYP2J6-specific peptide (QMEQNIMNRPLSVMQ) (Fig. 1) coupled to a carrier protein as the immunogen. This anti-CYP2J6pep IgG immunoreacted with microsomes of CYP2J6-expressing *Sf*9 cells to yield a prominent band with an estimated molecular mass of 55–57 kDa (Fig. 4B). The anti-CYP2J6pep did not cross-react with microsomes prepared from *Sf*9 cells expressing recombinant CYP2J5 (Fig. 4B), CYP2J2, CYP2J3, or CYP2J9 (data not shown), nor did it immunoreact with uninfected *Sf*9 cell microsomes (Fig. 4B).

CYP2J6 baculovirus-infected *Sf*9 cells were solubilized in a buffer containing the nonionic detergent Emulgen 911, and CO-difference spectra were obtained immediately. Fig. 5A shows one of those spectra that exhibits a Soret maxima at ~450 nm and a small peak at 420 nm. This spectrum is similar to that reported for other β-type cytochromes including CYP2J5 (Fig. 5D) and confirms that CYP2J6 is, in fact, a cytochrome P450. In most cases, however, the 420 nm peak was of higher intensity than the 450 nm peak, suggesting spontaneous conversion to a cytochrome P420-type pentacoordinate denatured form

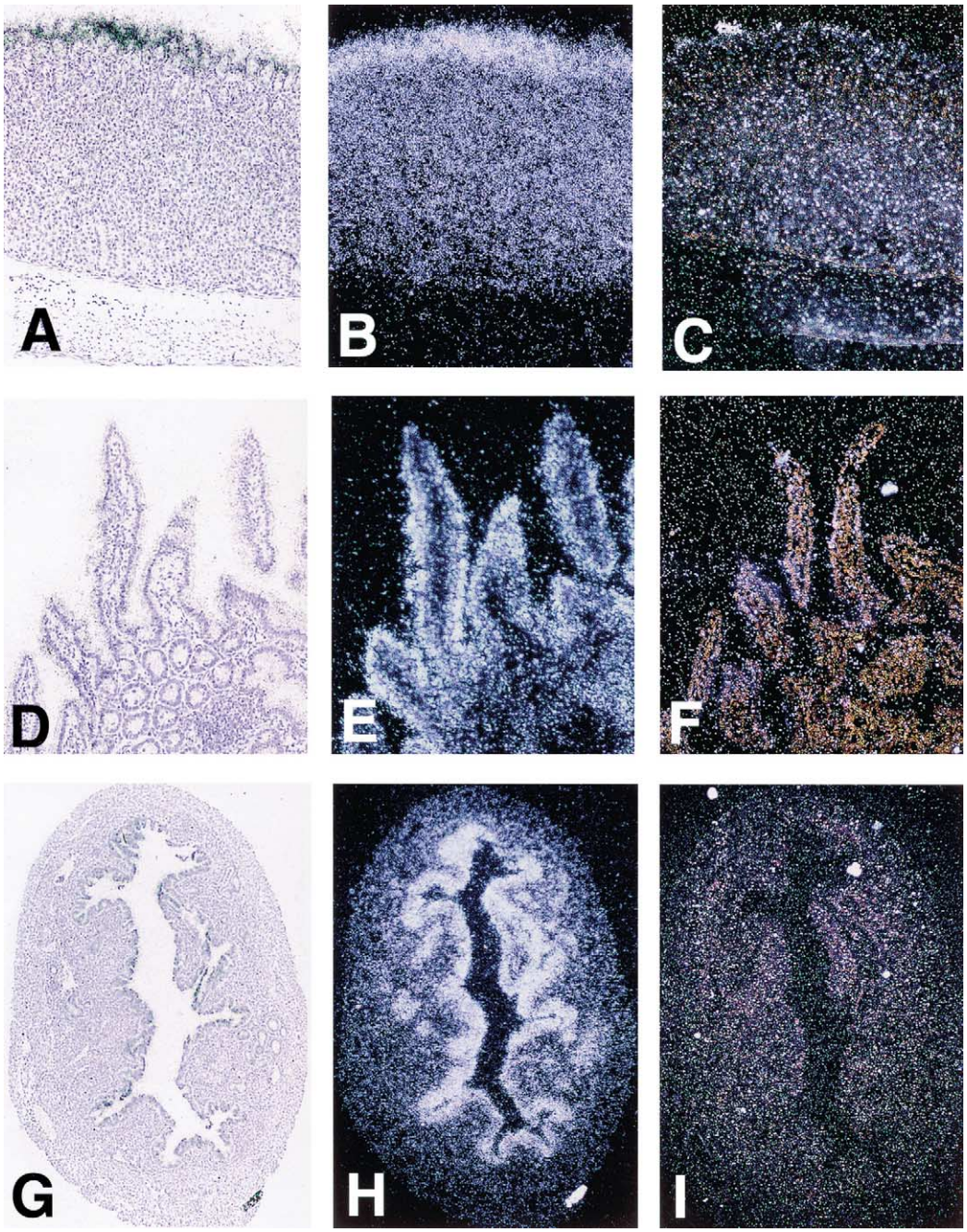

Fig. 3. Distribution of CYP2J6 RNAs by *in situ* hybridization. Mouse stomach (A–C), small intestine (D–F), and uterus (G–I) sections were stained with either ^{35}S-labeled antisense (A, B, D, E, G, and H) or sense (C, F, and I) CYP2J6 RNA probes and counterstained with hematoxylin as described in Section 2. Photomicrographs were taken at magnifications of 150× (A–F) or 60× (G–I) under brightfield (A, D, and G) or darkfield (B, C, E, F, H, and I) conditions. Results shown are representative of results from three animals.

of the enzyme. In fact, CO-difference spectra of microsomes prepared from CYP2J6-expressing *Sf*9 cells (Fig. 5C) were often similar to those observed for microsomes prepared from uninfected *Sf*9 cells (Fig. 5B), despite the presence of abundant CYP2J2- and CYP2J6-immunoreactive protein by western blotting (Fig. 4A and B).

To further characterize the stability of the CYP2J6 protein, we determined the effects of homogenization, sonication, repeated freezing/thawing, and lysis of CYP2J6-infected *Sf*9 cells in a sodium cholate-containing buffer on CO-difference spectra and CYP2J6 immunoreactive protein. Whereas these manipulations had little effect on spectra obtained from CYP2J5-infected *Sf*9 cells, CO-difference spectra from manipulated CYP2J6-infected *Sf*9 cells typically showed a prominent peak at 420 nm and an absence of a Soret maxima at 450 nm. Addition of 10–20% glycerol, protease inhibitors, P450 inhibitors (e.g. SKF525A), and/or P450 substrates (e.g. benzphetamine,

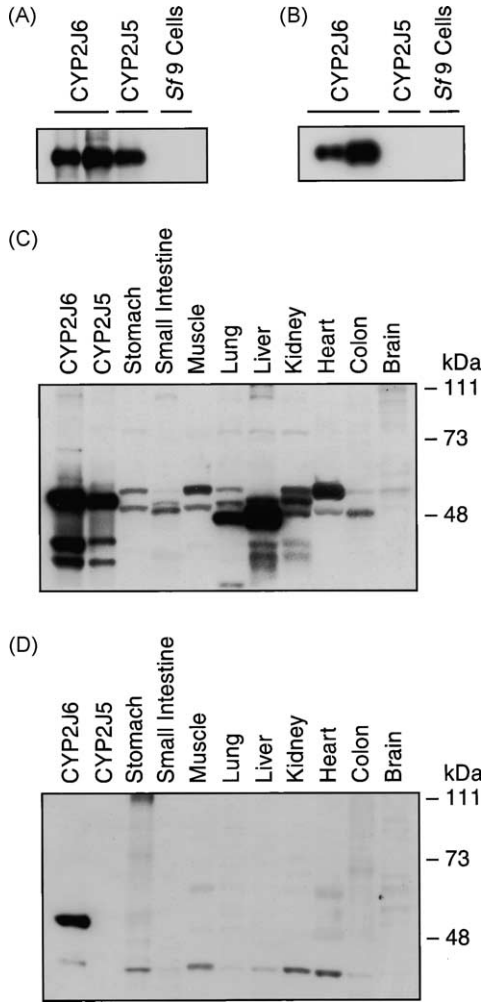

Fig. 4. Immunoblot analysis of recombinant CYP2J proteins and mouse tissue microsomes. Microsomal fractions prepared from uninfected *Sf*9 insect cells, *Sf*9 cells infected with recombinant CYP2J5 or CYP2J6 baculovirus stock (0.1 μg protein/lane), or mouse tissues (30–60 μg protein/lane) were electrophoresed on SDS–12% polyacrylamide gels, and the resolved proteins were transferred to nitrocellulose as described in Section 2. Membranes were immunoblotted with either anti-human CYP2J2 IgG (panels A and C) or anti-CYP2J6pep IgG (panels B and D), then goat anti-rabbit IgG conjugated to horseradish peroxidase, and finally immunoreactive proteins were visualized using the Amersham ECL detection system.

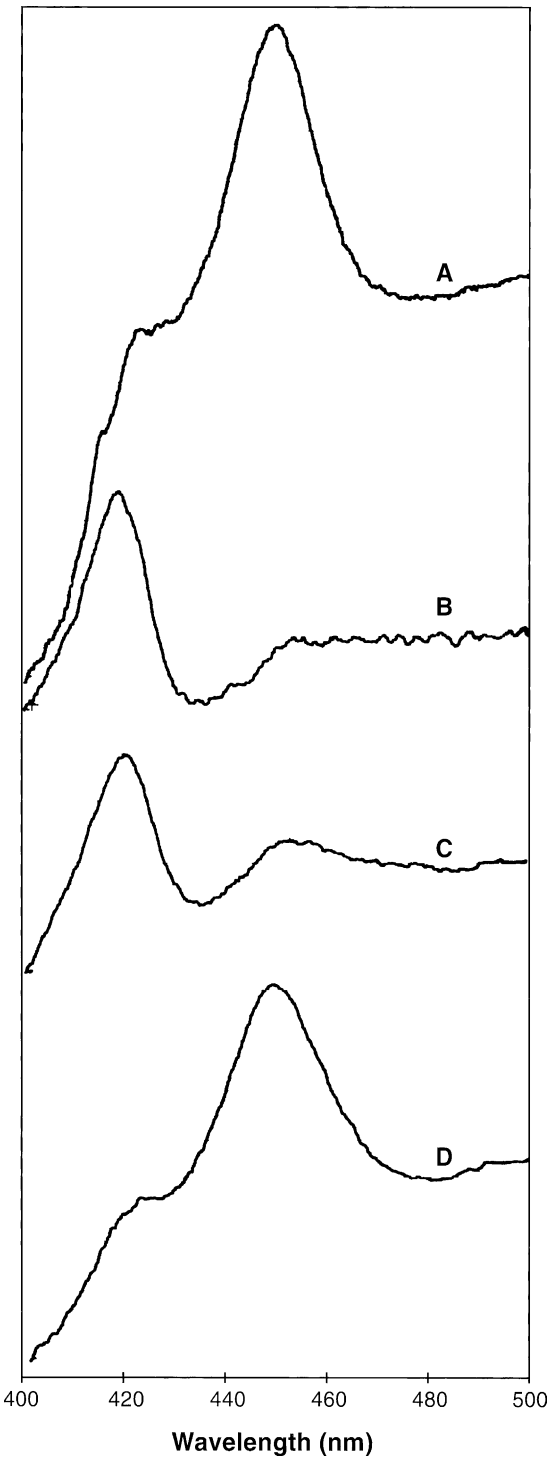

Fig. 5. CO-difference spectra of recombinant CYP2J6 protein. All spectra were recorded at room temperature as described in Section 2. (A) CYP2J6-expressing *Sf*9 insect cells solubilized with PGE lysis buffer. (B) Uninfected *Sf*9 cells solubilized with PGE lysis buffer. (C) Microsomes prepared from CYP2J6-expressing *Sf*9 insect cells. (D) Microsomes prepared from CYP2J5-expressing *Sf*9 insect cells. Ordinate, absorbance; abscissa, wavelength (nm).

arachidonic acid) to the cells prior to manipulation had no significant effect on these results. Furthermore, even in the presence of Emulgen 911, we observed a time-dependent reduction in the peak at 450 nm and a corresponding increase in the 420 nm peak that occurred within 1–2 hr at room temperature (Fig. 6) and within 4–6 hr at 4° (data not shown). Immunoblotting with the anti-CYP2J6pep IgG showed that the level of CYP2J6 immunoreactive protein was unaffected by these manipulations. Thus, the prominent 55–57 kDa band was unchanged when microsomes prepared from CYP2J6-infected *Sf*9 cells were subjected to as many as nine freeze–thaw cycles (Fig. 7A). Similarly, homogenization, sonication, or lysis in CYP2J6-expressing cells in sodium cholate-containing buffer had no effect on the abundance of CYP2J6 immunoreactive protein by western blotting (data not shown). However, we did observe that maintenance of CYP2J6-containing microsomes at room temperature for prolonged periods of time

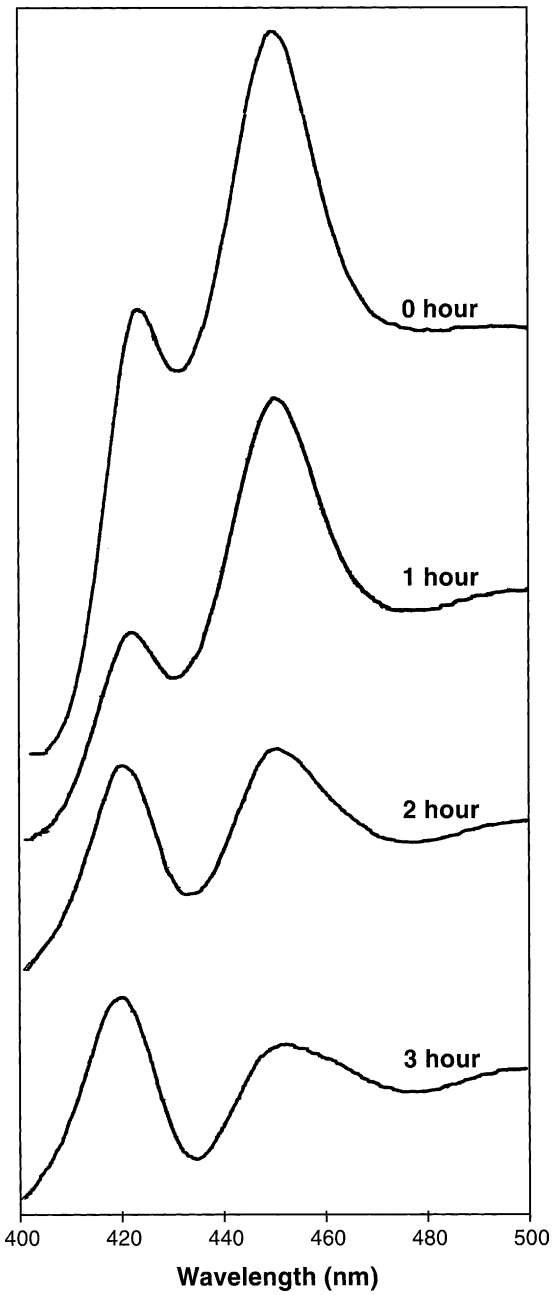

Fig. 6. CO-difference spectra showing instability of recombinant CYP2J6 protein. CYP2J6-expressing *Sf*9 insect cells were solubilized with PGE lysis buffer, and CO-difference spectra were recorded over 3 hr at room temperature as described in Section 2. Ordinate, absorbance; abscissa, wavelength (nm).

resulted in a gradual reduction in the amount of CYP2J6 immunoreactive protein (Fig. 7B). We also observed the presence of lower molecular mass bands (~25–30 kDa), although the intensity of these CYP2J6 immunoreactive proteins did not appear to change significantly with the various experimental manipulations (Fig. 7A and B). Taken together, these data suggest that CYP2J6 protein is unstable *in vitro*, undergoes rapid denaturation with minimal manipulation even in the presence of detergents and substrate, and degrades much more slowly.

3.5. Tissue distribution of CYP2J proteins in mouse

To examine the distribution of murine CYP2J proteins, we performed immunoblotting of microsomal fractions prepared from various mouse tissues using both the anti-CYP2J2 IgG and anti-CYP2J6pep IgG. As shown in Fig. 4C, the anti-CYP2J2 IgG produced a complex pattern, recognizing *at least* seven distinct proteins with molecular mass between 50 and 58 kDa. The slowest migrating band, with an estimated molecular mass of 58 kDa, was present in all tissues except liver and was most abundant in heart, kidney, and skeletal muscle. A band with an estimated molecular mass of 56 kDa, which co-migrated with recombinant CYP2J5 and CYP2J6, was present in liver and kidney but not in other mouse tissues including small intestine and colon. An ~55 kDa band was present in small intestine, lung, and brain. An ~54 kDa band was present in stomach and skeletal muscle. An ~53 kDa band was present most abundantly in liver and at lower levels in small intestine, kidney, heart, and colon. An ~52 kDa band was uniquely expressed in lung microsomes, and an ~50 kDa band was present only in liver. While the identity of the individual bands remains unknown, we conclude the following based on these data and on the known cross-reactivity of the anti-CYP2J2 IgG: (a) mouse microsomes contain multiple proteins that share immunologic properties with human CYP2J2; (b) mouse intestinal tissues contain at least three of these CYP2J2 immunoreactive proteins; and (c) only mouse liver and kidney contain a protein with electrophoretic properties identical to recombinant CYP2J5 and CYP2J6. Interestingly, the anti-CYP2J6pep IgG did not detect a protein with the same electrophoretic mobility as recombinant CYP2J6 in any of the mouse tissues examined (Fig. 4D). However, lower molecular mass bands in the ~25–30 kDa range were observed in all of the mouse tissues examined as well as in the recombinant CYP2J6 preparation (Fig. 4D). As in the case of the anti-CYP2J2 IgG immunoblot, the identity of these CYP2J6 immunoreactive bands remains unknown. Indeed, these lower molecular mass bands may be unrelated to CYP2J6.

The fact that the anti-CYP2J6pep IgG recognized the recombinant CYP2J6 protein in *Sf*9 cell extracts but did not detect a protein of the predicted molecular mass in mouse small intestinal microsomes, despite the abundance of CYP2J6 transcripts in mouse small intestinal RNA as indicated by northern blot and RT–PCR, suggested that the CYP2J6 protein was unstable *in vivo*. To address this issue further, we incubated recombinant CYP2J6 protein with mouse small intestinal cytosol, microsomes, or buffer for 1–24 hr at 37° and then immunoblotted the resulting proteins with the anti-CYP2J6pep IgG. We observed a significant loss of the prominent 55–57 kDa CYP2J6 band in 1- to 3-hr incubations containing microsomes, and, to a lesser extent, in incubations containing cytosol, but not in incubations containing buffer alone (Fig. 7C). Coincident with the reduction in the 55–57 kDa band was the appearance of

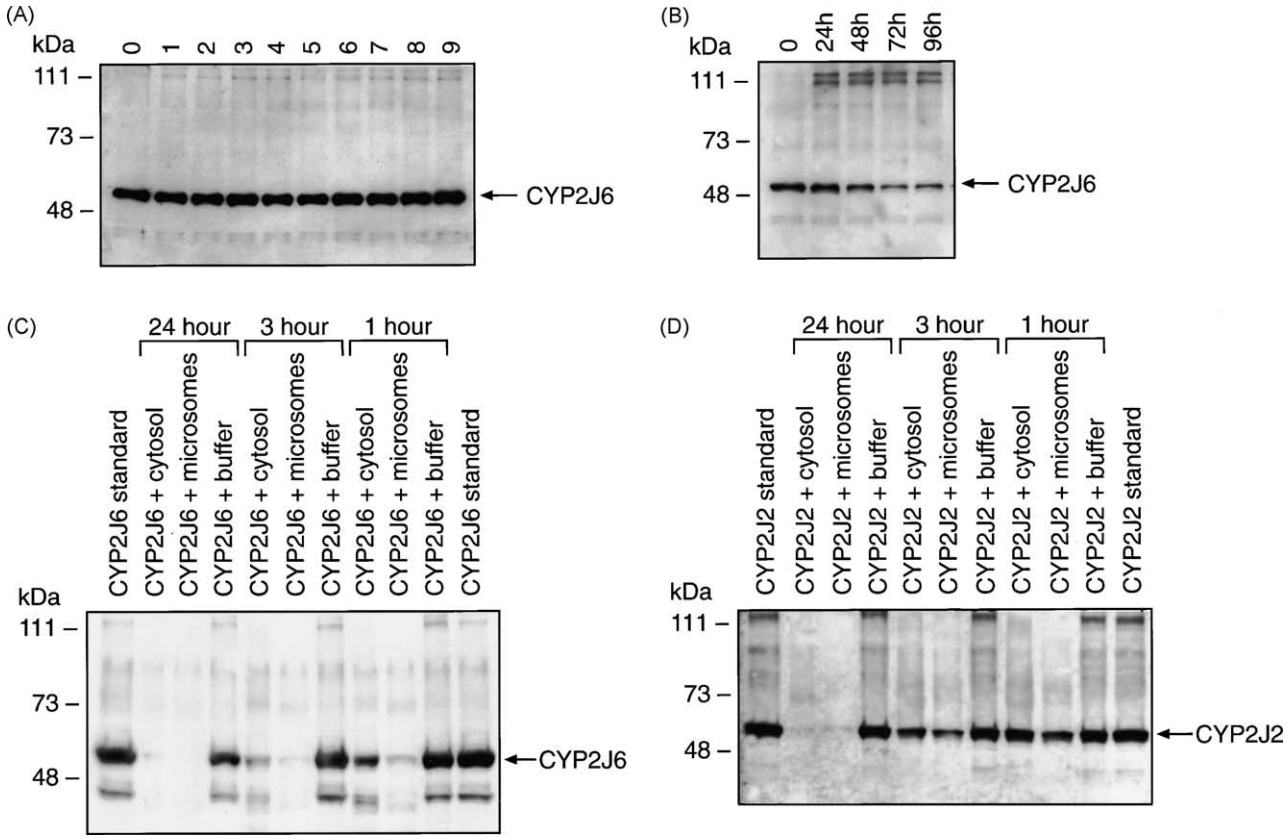

Fig. 7. Stability of CYP2J6 protein by immunoblot analysis. (A) Microsomal fractions prepared from *Sf*9 cells infected with recombinant CYP2J6 baculovirus were subjected to up to nine freeze–thaw cycles (number of cycles indicated above lane). Samples (0.1 μg protein/lane) were then electrophoresed on SDS–10% polyacrylamide gels, and the resolved proteins were transferred to nitrocellulose as described in Section 2. Membranes were immunoblotted with the anti-CYP2J6pep IgG, then goat anti-rabbit IgG conjugated to horseradish peroxidase, and finally immunoreactive proteins were visualized using the ECL detection system. (B) Microsomes prepared from CYP2J6-expressing *Sf*9 insect cells were incubated at room temperature for up to 96 hr prior to immunoblotting as described for panel A. (C) Microsomes prepared from CYP2J6-expressing *Sf*9 insect cells were incubated with mouse small intestinal microsomes, cytosol, or buffer at 37° for 1–24 hr prior to immunoblotting as described for panel A. (D) Microsomes prepared from CYP2J2-expressing *Sf*9 insect cells were incubated with mouse small intestinal microsomes, cytosol, or buffer at 37° for 1–24 hr prior to immunoblotting with the anti-human CYP2J2 IgG.

several lower molecular mass proteins consistent with degradation of the CYP2J6 protein at several proteolytic sites. By 24 hr, no significant CYP2J6 protein was evident in the cytosolic and microsomal incubates. In contrast, we did not observe similar degradation during 1- to 3-hr incubations of recombinant human CYP2J2 protein with small intestinal microsomes, cytosol, or buffer; However, significant degradation of CYP2J2 was evident by 24 hr (Fig. 7D). These data provide evidence that CYP2J6 is degraded rapidly in the presence of small intestinal microsomes and cytosol, and is consistent with post-translational modification of endogenous intestinal CYP2J6 protein due to proteolysis at highly sensitive sites.

Recently, Xie and co-workers [27] reported induction of a CYP2J4-immunoreactive protein in multiple mouse tissues following intraperitoneal administration of pyrazole. To determine if CYP2J6 is a pyrazole-inducible P450, we treated mice with pyrazole for 3 days and then performed immunoblots on microsomal fractions prepared from multiple tissues with the anti-CYP2J6pep IgG. The antibody did not detect any proteins with an electrophoretic mobility similar to recombinant CYP2J6 in small intestine, heart, liver, or kidney microsomes prepared from pyrazole-treated mice (data not shown). Moreover, the intensity of the 25–30 kDa CYP2J6-immunreactive bands remained unchanged compared with vehicle-treated mice. Based on these data, we conclude that it is unlikely that mouse CYP2J6 is inducible by pyrazole, at least under the experimental conditions that we employed. It remains possible that pyrazole induced CYP2J6 but that it either was degraded rapidly in the small intestine or else its levels remained below the detection limit of our western blot assay.

3.6. Enzymatic characterization of recombinant CYP2J6

Microsomes prepared from *Sf*9 cells co-expressing CYP2J6 and CYPOR were inactive in the metabolism of both benzphetamine and arachidonic acid, presumably due to the *in vitro* instability of the recombinant CYP2J6 protein. However, we did perform incubations of live *Sf*9 cells co-expressing recombinant CYP2J6 and CYPOR with the two known CYP2J substrates. CYP2J6-expressing *Sf*9 cells actively metabolized benzphetamine to formaldehyde (catalytic turnover: 23 pmol product formed/10^6 cells/min

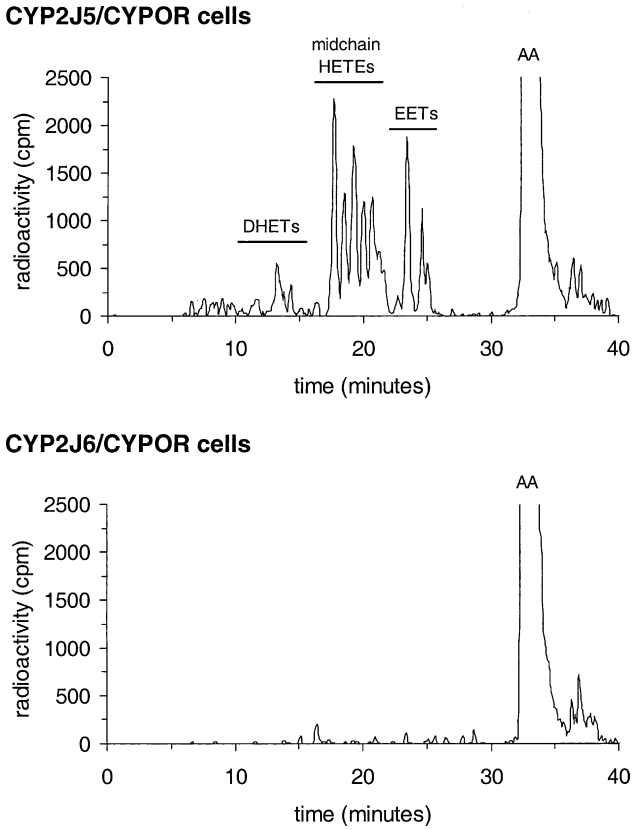

Fig. 8. Metabolism of arachidonic acid (AA) by *Sf*9 cells expressing recombinant CYP2J5 and CYP2J6. Reverse-phase HPLC chromatograms of organic soluble metabolites generated during incubation of *Sf*9 cells co-expressing CYP2J5 and CYPOR (top panel) or *Sf*9 cells co-expressing CYP2J6 and CYPOR (bottom panel) with [1-^{14}C]arachidonic acid. Products were identified by comparing their HPLC properties with those of authentic standards. DHETs = dihydroxyeicosatrienoic acids.

at 37°). For comparison, uninfected *Sf*9 cells and *Sf*9 cells expressing CYPOR but no P450 metabolized benzphetamine at a background rate of <5 pmol product formed/10^6 cells/min at 37°, and *Sf*9 cells co-expressing CYP2J3 and CYPOR metabolized benzphetamine at a rate of 59 pmol product formed/10^6 cells/min. In contrast, we observed no significant metabolism of arachidonic acid by the CYP2J6-CYPOR infected *Sf*9 cells (Fig. 8, bottom panel). Under identical reaction conditions, *Sf*9 cells co-expressing recombinant CYP2J5 and CYPOR rapidly metabolized arachidonic acid to EETs and midchain HETEs (Fig. 8, top panel). Based on these data, we conclude that benzphetamine is a substrate for CYP2J6 whereas arachidonic acid is not.

4. Discussion

Intestinal P450s have been proposed to play important roles in the biotransformation of ingested xenochemicals and in the activation or detoxification of chemical carcinogens in this tissue [19]. Members of the CYP1A, CYP2B, CYP2C, CYP2D, CYP2E, and CYP3A subfamilies have been shown to be constitutively expressed in the intestine [28–34]. In addition, CYP2J subfamily members are abundant in intestinal tissue, and in the case of rabbit CYP2J1 and rat CYP2J4, are expressed predominantly in the small intestine [2–6,17,20–22]. Herein, we report the cDNA cloning, heterologous expression, and functional characterization of a new mouse P450 (CYP2J6) that is abundant in the small intestine, expressed primarily in luminal epithelial cells, and active in the metabolism of benzphetamine to formaldehyde. We demonstrated that, unlike other members of this subfamily, mouse CYP2J6 is unstable *in vitro* and undergoes rapid denaturation with minimal manipulation. We also provide immunologic data to show that several CYP2J immunoreactive proteins are contained in the mouse.

One question that remains is whether or not mouse CYP2J6 is orthologous to rat CYP2J4. On the one hand, CYP2J4 and CYP2J6 are 94% identical at the amino acid level, most of the differences represent conservative amino acid substitutions, and with the exception of amino acid 121, the two heme-thiolate proteins have identical sequences within the six putative substrate recognition sites [6,35]. However, Nelson *et al.* [1,36] have suggested that similarities in amino acid sequence alone cannot be used to determine orthologous genes across species or to classify genes within a given subfamily. In some cases, regulatory features or cDNA-expressed catalytic activities have been used to ascertain orthologous P450 genes between species [37]. While both CYP2J4 and CYP2J6 mRNAs are expressed primarily in the small intestine, CYP2J4 is up-regulated by pyrazole [22,27], whereas we detected no such up-regulation with a specific CYP2J6 antibody in mouse tissues. Moreover, CYP2J4 and CYP2J6 appear to be enzymologically distinct proteins in that CYP2J4 is active in arachidonic acid metabolism [6], whereas we observed no significant metabolism of this substrate by recombinant CYP2J6. Likewise, CYP2J6 is active in the metabolism of benzphetamine, while aromatic amines have not been reported to be substrates for CYP2J4 [6,9,17,22]. In several multi-gene subfamilies (e.g. CYP2A, CYP2B, CYP2C, and CYP4A), numerous species-specific gene duplication, unequal crossing-over, and gene conversion events have made orthologue assignments between species impossible [1,37]. The documentation of multiple genes within the mouse CYP2J subfamily [7,8] suggests a complexity that makes the classification of proteins encoded by these genes difficult.

We observed a spontaneous disappearance of the Soret peak at 450 nm in the CO-difference spectrum of reduced CYP2J6 and the subsequent appearance of a prominent peak at 420 nm. This conversion to the cytochrome P420 form suggests an unstable enzyme having the thiolate of cysteine displaced from the 5th position of the heme iron. The half-life of this spectral conversion was relatively rapid, even in the presence of detergent or substrate. Similar spontaneous spectral conversions have been reported for other

P450s including the mouse testosterone 7α-hydroxylase (CYP2A12), allelic variants of CYP2D6 and CYP4A11, and most recently for the neuronal isoform of nitric oxide synthase [38–41]. In some of these cases (e.g. CYP2A12), stability was enhanced by the addition of substrate, and the enzyme was active. In others (e.g. CYP4A11v), the enzyme remained relatively inactive despite the presence of substrate. We found that despite rapid conversion to the pentacoordinate denatured form, CYP2J6 protein degradation, as assessed by immunoblotting, occurred relatively slowly. Interestingly, we observed rapid degradation of the recombinant CYP2J6 protein in the presence of small intestinal microsomes and, to a lesser extent, in the presence of small intestinal cytosol. Moreover, the antibody did not detect a protein with the same electrophoretic mobility as recombinant CYP2J6 in any of the mouse tissues examined. Together, these data are consistent with proteolysis of endogenous CYP2J6 at highly sensitive sites.

Northern analysis demonstrated that CYP2J6 transcripts are most abundant in the small intestine but also present in several other mouse tissues including liver, kidney, colon, brain, heart, and lung. The widespread tissue distribution of CYP2J6 transcripts was confirmed independently by RT–PCR. Recently, Xie and co-workers [27] used a combination of RT–PCR and restriction mapping of CYP2J-related DNA fragments to document the broad tissue distribution of CYP2J6 mRNAs. Those investigators also used a polyclonal antibody to rat CYP2J4 and showed that CYP2J4-related proteins were present in all mouse tissues examined [27]. Given the high degree of similarity between rat CYP2J4 and mouse CYP2J6, it is possible that the signals detected on their immunoblots represent CYP2J6. However, the protein that Xie and co-workers detected was pyrazole-inducible, and our own immunoblotting data with the anti-CYP2J6pep IgG did not reveal any pyrazole-inducible proteins. Thus, further work will be necessary to conclusively identify the pyrazole-inducible protein detected by Xie *et al*. In light of the marked instability of the CYP2J6 protein in the presence of small intestinal microsomes and cytosol, any statements regarding the tissue distribution and/or inducibility of this P450 must be interpreted with caution.

We have provided immunologic data herein to support the complexity of the murine CYP2J subfamily. Western blots using an antibody to purified, recombinant human CYP2J2 demonstrate the presence of multiple proteins in mouse tissues that are immunologically related to the CYP2Js. The intestine alone appears to contain *at least* three distinct CYP2J immunoreactive proteins. In this regard, Koike *et al.* [20] recently purified two P450s belonging to the CYP2J subfamily from rabbit small intestine, and Zhang and co-workers [6] demonstrated that rat enterocytes contain two proteins that immunoreact with a CYP2J4 peptide-based antibody.

Exposure to xenochemicals such as aromatic amines from occupational and/or environmental sources has long been recognized as a risk factor for cancer [19,42,43]. The gastrointestinal tract represents a major portal of entry for such compounds, either via ingestion or secondarily by swallowing inhaled xenobiotics that have been cleared from the tracheobronchial tree. Thus, the intestinal P450 monooxygenases represent the initial enzyme system involved in the biotransformation of these potentially harmful chemicals, an event that can lead to their detoxification/excretion and/or toxification/activation [19,42,43]. Our findings here that CYP2J6 mRNA is highly expressed in intestinal epithelia and that the recombinant protein is active in the metabolism of the aromatic amine benzphetamine to formaldehyde suggest one potential functional role of this P450. An interesting finding is the expression of CYP2J6 mRNAs within the female mouse uterus, mostly within the luminal epithelium and in endometrial glands. Cytochrome P450 enzymes that are involved in the production and/or metabolism of steroid hormones are known to be expressed within the uterus and have been proposed to play a role in the regulation of estrogenic effects [44,45]. Others have reported expression of xenobiotic-metabolizing P450s (including CYP1A1 and CYP1B1) within the human uterus and have proposed that variability in their expression may be responsible for the differential susceptibility to uterine cancer [46]. Further work will be necessary to determine if this enzyme also plays a role in the metabolism of steroids and/or chemical carcinogens within the female reproductive tract.

We used an antisense RNA probe to the full-length CYP2J6 subjected to alkaline hydrolysis for *in situ* hybridization experiments. While it is possible that there was some cross-hybridization with other mouse CYP2J transcripts under our experimental conditions, none of the other known murine CYP2Js are expressed significantly in the small intestine or uterus [7–9]. Nevertheless, we recommend caution in the interpretation of our data on the cellular localization of CYP2J6 in these tissues.

In summary, we report the cDNA cloning and heterologous expression of a new mouse P450, CYP2J6, whose transcripts are abundant in the small intestine and are expressed predominantly in luminal epithelial cells. The recombinant CYP2J6 protein is active in the metabolism of benzphetamine but is unstable *in vitro*. Unlike other members of the CYP2J subfamily, CYP2J6 does not appear to be active in the metabolism of arachidonic acid. Finally, we provide immunologic evidence for the presence of multiple CYP2J mouse isoforms. We conclude that CYP2J6 is an unstable mouse P450 active in the metabolism of benzphetamine and that the mouse CYP2J subfamily is complex.

Acknowledgments

The authors wish to thank Dr. Cosette Sirabjit-Singh (GlaxoSmithKline) for providing the original pAcUW51-CYPOR construct. We are also indebted to Drs. Joyce

Goldstein and Tom Eling for their helpful suggestions during the preparation of this manuscript. This work was supported by the National Institutes of Environmental Health Sciences Division of Intramural Research and NIH 2 P01-DK38266 (to M.D.B.). Portions of this work were presented at the 17th International Congress of Biochemistry and Molecular Biology, San Francisco, CA.

References

[1] Nelson DR, Koymans L, Kamataki T, Stegeman JJ, Feyereisen R, Waxman DJ, Waterman MR, Gotoh O, Coon MJ, Estabrook RW, Gunsalus IC, Nebert DW. P450 superfamily: update on new sequences, gene mapping, accession numbers and nomenclature. Pharmacogenetics 1996;6:1–42.

[2] Ichihara K, Kusunose E, Kaku M, Yamamoto S, Kusunose M. Separation of two constitutive forms of cytochrome *P*-450 active in aminopyrine *N*-demethylation from rabbit intestinal mucosa microsomes. Biochim Biophys Acta 1985;831:99–105.

[3] Kikuta Y, Sogawa K, Haniu M, Kinosaki M, Kusunose E, Nojima Y, Yamamoto S, Ichihara K, Kusunose M, Fujii-Kuriyama Y. A novel species of cytochrome P-450 ($P\text{-}450_{ib}$) specific for the small intestine of rabbits. cDNA cloning and its expression in COS cells. J Biol Chem 1991;266:17821–5.

[4] Wu S, Moomaw CR, Tomer KB, Falck JR, Zeldin DC. Molecular cloning and expression of CYP2J2, a human cytochrome P450 arachidonic acid epoxygenase highly expressed in heart. J Biol Chem 1996;271:3460–8.

[5] Wu S, Chen W, Murphy E, Gabel S, Tomer KB, Foley J, Steenbergen C, Falck JR, Moomaw CR, Zeldin DC. Molecular cloning, expression, and functional significance of a cytochrome P450 highly expressed in rat heart myocytes. J Biol Chem 1997;272:12551–9.

[6] Zhang Q-Y, Ding X, Kaminsky LS. Cloning, heterologous expression, and characterization of rat intestinal CYP2J4. Arch Biochem Biophys 1997;340:270–8.

[7] Ma J, Qu W, Scarborough PE, Tomer KB, Moomaw CR, Maronpot R, Davis LS, Breyer MD, Zeldin DC. Molecular cloning, enzymatic characterization, developmental expression, and cellular localization of a mouse cytochrome P450 highly expressed in kidney. J Biol Chem 1999;274:17777–88.

[8] Qu W, Bradbury JA, Tsao CC, Maronpot R, Harry GJ, Parker CE, Davis LS, Breyer MD, Waalkes MP, Falck JR, Chen J, Rosenberg RL, Zeldin DC. Cytochrome P450 CYP2J9, a new mouse arachidonic acid ω-1 hydroxylase predominately expressed in brain. J Biol Chem 2001;276:25467–79.

[9] Scarborough PE, Ma J, Qu W, Zeldin DC. P450 subfamily CYP2J and their role in the bioactivation of arachidonic acid in extrahepatic tissues. Drug Metab Rev 1999;31:205–34.

[10] Falck JR, Manna S, Moltz J, Chacos N, Capdevila J. Epoxyeicosatrienoic acids stimulate glucagon and insulin release from isolated rat pancreatic islets. Biochem Biophys Res Commun 1983;114:743–9.

[11] Capdevila J, Chacos N, Falck JR, Manna S, Negro-Vilar A, Ojeda SR. Novel hypothalamic arachidonate products stimulate somatostatin release from the median eminence. Endocrinology 1983;113:421–3.

[12] Proctor KG, Falck JR, Capdevila J. Intestinal vasodilation by epoxyeicosatrienoic acids: arachidonic acid metabolites produced by a cytochrome P450 monooxygenase. Circ Res 1986;60:50–9.

[13] Gebremedhin D, Ma Y-H, Falck JR, Roman RJ, VanRollins M, Harder DR. Mechanism of action of cerebral epoxyeicosatrienoic acids on cerebral arterial smooth muscle. Am J Physiol 1992;263: H519–25.

[14] Zeldin DC, Plitman JD, Kobayashi J, Miller RF, Snapper JR, Falck JR, Szarek JL, Philpot RM, Capdevila JH. The rabbit pulmonary cytochrome P450 arachidonic acid metabolic pathway: characterization and significance. J Clin Invest 1995;95:2150–60.

[15] Pascual MMS, McKenzie A, Yankaskas JR, Zeldin DC. Epoxygenase metabolites of arachidonic acid affect electrophysiologic properties of rat tracheal epithelial cells. J Pharmacol Exp Ther 1998;286:772–9.

[16] Node K, Huo Y, Ruan X, Yang B, Spiecker M, Ley K, Zeldin DC, Liao JK. Anti-inflammatory properties of cytochrome P450 epoxygenase-derived eicosanoids. Science 1999;285:1276–9.

[17] Zhang Q-Y, Raner G, Ding X, Dunbar D, Coon MJ, Kaminsky LS. Characterization of the cytochrome P450 CYP2J4: expression in rat small intestine and role in retinoic acid biotransformation from retinal. Arch Biochem Biophys 1998;353:257–64.

[18] Moran JH, Mitchell LA, Bradbury JA, Ma J, Qu W, Schnellmann RG, Zeldin DC, Grant DF. Analysis of the cytotoxic properties of linoleic acid metabolites produced by P450s localized in renal tissues. Toxicol Appl Pharmacol 2000;168:268–79.

[19] Kaminsky LS, Fasco MJ. Small intestinal cytochrome P450. Crit Rev Toxicol 1992;21:407–22.

[20] Koike K, Kusunose E, Nishikawa Y, Ichihara K, Inagaki S, Takagi H, Kikuta Y, Kusunose M. Purification and characterization of rabbit small intestinal cytochromes belonging to CYP2J and CYP4A subfamilies. Biochem Biophys Res Commun 1997;232:643–7.

[21] Zeldin DC, Foley J, Goldsworthy SM, Cook ME, Boyle JE, Ma J, Moomaw CR, Tomer KB, Steenbergen C, Wu S. CYP2J subfamily P450s in the gastrointestinal tract: expression, localization, and potential functional significance. Mol Pharmacol 1997;51:931–43.

[22] Zhang Q-Y, Ding X, Dunbar D, Cao L, Kaminsky LS. Induction of rat small intestinal cytochrome P450 2J4. Drug Metab Dispos 1999;27:1123–7.

[23] Omura T, Sato R. The carbon monoxide binding pigment of liver microsomes. J Biol Chem 1964;239:2370–8.

[24] Maniatis TJ, Sambrook J, Fritsch EF. Molecular cloning: a laboratory manual. 2nd ed. Cold Spring Harbor, NY: Cold Spring Harbor Laboratory; 1989.

[25] Breyer MD, Jacobson HR, Davis LS, Breyer RM. *In situ* hybridization and localization of mRNA for the rabbit prostaglandin EP_3 receptor. Kidney Int 1993;44:1372–8.

[26] Nash T. The colorimetric estimation of formaldehyde by means of the Hantzsch reaction. Biochem J 1953;55:416–21.

[27] Xie Q, Zhang Q-Y, Zhang Y, Su T, Gu J, Kaminsky LS, Ding X. Induction of mouse CYP2J by pyrazole in the eye, kidney, liver, lung, olfactory mucosa, and small intestine, but not in the heart. Drug Metab Dispos 2000;28:1311–6.

[28] de Waziers I, Cugnenc PH, Yang CS, Leroux J-P, Beaune PH. Cytochrome P-450 isoenzymes, epoxide hydrolase and glutathione transferases in rat and human hepatic and extrahepatic tissues. J Pharmacol Exp Ther 1990;253:387–94.

[29] Peters WHM, Kremers PG. Cytochromes P-450 in the intestinal mucosa of man. Biochem Pharmacol 1989;38:1535–8.

[30] Murray GI, Barnes TS, Sewell HF, Ewen SWB, Melvin WT, Burke MD. The immunocytochemical localization and distribution of cytochrome P450 in normal human hepatic and extrahepatic tissues with a monoclonal antibody to human cytochrome P450. Br J Clin Pharmacol 1988;25:465–75.

[31] Watkins PB, Wrighton SA, Schuetz EG, Molowa DT, Guzelian PS. Identification of glucocorticoid-inducible cytochrome P450 in the intestinal mucosa of rats and man. J Clin Invest 1987;80:1029–36.

[32] Fasco MJ, Silkworth JB, Dunbar DA, Kaminsky LS. Rat small intestinal cytochrome P450 probed by warfarin metabolism. Mol Pharmacol 1993;43:226–33.

[33] Rich KJ, Sesardic D, Foster JR, Davies DS, Boobis AR. Immunohistochemical localization of cytochrome P450b/e in hepatic and extrahepatic tissues of the rat. Biochem Pharmacol 1989;38:3305–22.

[34] Shimizu M, Lasker JM, Tsutsumi M, Lieber CS. Immunohistochemical localization of ethanol-inducible P450IIE1 in the rat alimentary tract. Gastroenterology 1990;99:1044–53.

[35] Gotoh O. Substrate recognition sites in cytochrome P450 family 2 (CYP2) proteins inferred from comparative analyses of amino acid and coding nucleotide sequences. J Biol Chem 1992;267:83–90.
[36] Nelson DR, Kamataki T, Waxman DJ, Guengerich FP, Estabrook RW, Feyereisen R, Gonzalez FJ, Coon MJ, Gunsalus IC, Gotoh O, Okuda K, Nebert DW. The P450 superfamily: update on new sequences, gene mapping, accession numbers, early trivial names of enzymes, and nomenclature. DNA Cell Biol 1993;12:1–51.
[37] Nebert DW, Nelson DR. P450 gene nomenclature based on evolution. Methods Enzymol 1991;206:3–11.
[38] Imaoka S, Ogawa H, Kimura S, Gonzalez FJ. Complete cDNA sequence and cDNA-directed expression of CYP4A11, a fatty acid ω-hydroxylase expressed in human kidney. DNA Cell Biol 1993;12:893–9.
[39] Iwasaki M, Lindberg RLP, Juvonen RO, Negishi M. Site-directed mutagenesis of mouse steroid 7α-hydroxylase (cytochrome P-450$_{7\alpha}$): role of residue-209 in determining steroid-cytochrome P-450 interaction. Biochem J 1993;291:569–73.
[40] Aklillu E, Persson I, Bertilsson L, Johansson I, Rodrigues F, Ingelman-Sundberg M. Frequent distribution of ultrarapid metabolizers of dibrisoquine in an Ethiopian population carrying duplicated and multiduplicated functional CYP2D6 alleles. J Pharmacol Exp Ther 1996;278:441–6.
[41] Migita CT, Solerno JC, Masters BSS, Martasek P, McMillan K, Ikeda-Saito M. Substrate binding-induced changes in the EPR spectra of the ferrous nitric oxide complexes of neuronal nitric oxide synthase. Biochemistry 1997;36:10987–92.
[42] Hoensch HP, Hartmann F. The intestinal enzymatic biotransformation system: potential role in the protection from colon cancer. Hepatogastroenterology 1981;28:221–8.
[43] Laitinen M, Watkins JB. Mucosal biotransformations. In: Rozman K, Hanninen O, editors. Gastrointestinal toxicology. New York: Elsevier Science Publishers; 1986, p. 169–92.
[44] Schiff R, Arensburg J, Itin A, Keshet E, Orly J. Expression and cellular localization of uterine side-chain cleavage cytochrome P450 messenger ribonucleic acid during early pregnancy in mice. Endocrinology 1993;133:529–37.
[45] Zhu BT, Conney AH. Functional role of estrogen metabolism in target cells: review and perspectives. Carcinogenesis 1998;19:1–27.
[46] Vadlamuri SV, Glover DD, Turner T, Sarkar MA. Regiospecific expression of cytochrome P4501A1 and 1B1 in human uterine tissue. Cancer Lett 1998;122:143–50.